Surface loss simulations of superconducting coplanar waveguide resonators

J. Wenner, R. Barends, R. C. Bialczak, Yu Chen, J. Kelly, Erik Lucero, Matteo Mariantoni, A. Megrant, P. J. J. O'Malley, D. Sank, A. Vainsencher, H. Wang, T. C. White, Y. Yin, J. Zhao, A. N. Cleland, and John M. Martinis
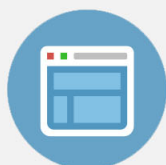
Surface loss simulations of superconducting coplanar waveguide resonators

J. Wenner,[1] R. Barends,[1] R. C. Bialczak,[1] Yu Chen,[1] J. Kelly,[1] Erik Lucero,[1] Matteo Mariantoni,[1] A. Megrant,[1] P. J. J. O'Malley,[1] D. Sank,[1] A. Vainsencher,[1] H. Wang,[1,2] T. C. White,[1] Y. Yin,[1] J. Zhao,[1] A. N. Cleland,[1] and John M. Martinis[1,a]

[1]*Department of Physics, University of California, Santa Barbara, California 93106, USA*
[2]*Department of Physics, Zhejiang University, Hangzhou 310027, China*

Losses in superconducting planar resonators are presently assumed to predominantly arise from surface-oxide dissipation, due to experimental losses varying with choice of materials. We model and simulate the magnitude of the loss from interface surfaces in the resonator and investigate the dependence on power, resonator geometry, and dimensions. Surprisingly, the dominant surface loss is found to arise from the metal-substrate and substrate-air interfaces. This result will be useful in guiding device optimization, even with conventional materials. © *2011 American Institute of Physics*. [doi:10.1063/1.3637047]

Superconducting coplanar waveguide (CPW) resonators are critical elements in photon detection,[1] quantum computation,[2–5] and creating and decohering quantum photon states.[6,7] Such applications are limited by the energy decay time. A prominent resonator decoherence source at low powers has previously been found to be two-level states (TLSs) on the various surfaces.[8–12] Knowing TLS locations is important to improve the resonators. Previous measurements and simulations suggested that the exposed metal surface (metal-air interface) is a crucial decoherence source,[9–11] driving research in using non-oxidizing superconductors for quantum devices. However, we show with simulations and a model that, for typical metal oxide parameters, the more likely source of CPW loss is instead the metal-substrate and substrate-air interfaces, changing the approach needed to reduce losses.

Thin-film resonators have three types of amorphous interfaces that can contain TLSs and thus introduce surface losses (Fig. 1): metal-air (ma), metal-substrate (ms), and substrate-air (sa). Each interface can include a thin oxide or contaminant layer sandwiched between the two primary layers. The total loss tangent for these thin layers is $\sum_i p_i \tan \delta_i$, where surface interface type i has loss tangent $\tan \delta_i$ and participation ratio[8,13]

$$p_i = W^{-1} t_i \epsilon_i \int ds |E|^2, \qquad (1)$$

for thickness t_i, dielectric constant ϵ_i, length coordinate s, and energy per unit length W. Using the boundary conditions on the electric displacement gives the three interface participation ratios:[14]

$$p_{\mathrm{ma}} W / t_{\mathrm{ma}} = \epsilon_{\mathrm{ma}}^{-1} \int ds |E_{\mathrm{a}\perp}|^2, \qquad (2)$$

$$p_{\mathrm{ms}} W / t_{\mathrm{ms}} = (\epsilon_{\mathrm{s}}^2 / \epsilon_{\mathrm{ms}}) \int ds |E_{\mathrm{s}\perp}|^2, \qquad (3)$$

$$p_{\mathrm{sa}} W / t_{\mathrm{sa}} = \epsilon_{\mathrm{sa}} \int ds |E_{\mathrm{a}\|}|^2 + \epsilon_{\mathrm{sa}}^{-1} \int ds |E_{\mathrm{a}\perp}|^2, \qquad (4)$$

where E_{a} (E_{s}) is the electric field in the air (substrate) outside the interface and $E_{\|}$ ($E_{\perp}$) is the electric field component parallel (perpendicular) to the interface.

Here, we take all dielectric constants to be of order $\epsilon \sim 10$, typical of metal oxides. Then, p_{ma} and $p_{\mathrm{sa},\perp}$ are of order 1% of p_{ms} and $p_{\mathrm{sa},\|}$. Thus, if all interface loss tangents and thicknesses are similar, the substrate-air and metal-substrate interfaces are 100 times more lossy than the metal-air interface.

To accurately compare to this model, we numerically calculated the participation ratios with the finite-element solver COMSOL (Ref. 15), using Eqs. (2)–(4) to extract the participation ratios from surface fields.[14] To obtain rough estimates of the loss, we used interface parameters typical of chemi- or physisorbed water or organics,[14,16] $t = 3$ nm and $\tan \delta \sim 0.002$, changing these rescale participation ratios according to Eqs. (2)–(4). As shown in Table I, p_{ma} is 40–60 times smaller than p_{ms} and p_{sa}, validating the discussion above. In addition, typical measured quality factors are 10^5, much closer to the predictions for the metal-substrate and substrate-air interfaces than the 10^7 for the metal-air interface.
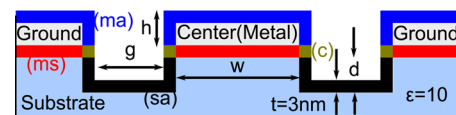

FIG. 1. (Color online) Coplanar waveguide dimensions and interfaces. Dimensions are the center width w, gap width g, metal height h, etch depth d, and assumed interface thickness $t = 3$ nm. This structure has metal-air (ma), metal-substrate (ms), and substrate-air (sa) interfaces. The 3 nm × 3 nm corner square (c) is treated separately.

[a]Electronic mail: martinis@physics.ucsb.edu.

Participation ratios dominate contributions from the edges around the coplanar gap;[14] the scaling of the electric fields with distance is displayed in Fig. 2. For distances r from corners much greater than other relevant dimensions, the field scales as $r^{-1/2}$, the predicted scaling for the field from a flat edge.[17] The electric fields on the metal-air interface and on the unetched metal-substrate interface scale as $r^{-1/3}$, the predicted behavior for the field from a metal 90° corner;[17] here, 20% of the participation ratio is within 1% of the length at the edge. Hence, we also calculate the participation ratio p_c for a 3 nm square at metal-air-substrate corners (as shown in Fig. 1) and find the loss from this small corner is only 3–4 times smaller than from the metal-air and substrate-air interfaces.

Etching the substrate in the coplanar gap flattens the field dependence on r at the metal-air-substrate corner (Fig. 2). This implies etching the substrate significantly reduces p_c while leaving p_{ma} and p_{ms} unchanged, along with a potential decrease in p_{sa} due to lower surface fields. Remarkably, even a 10 nm etch reduces p_c by 70%, while a 2 μm etch reduces p_c by 99% along with p_{sa} by 50%.

The microstrip geometry also changes the participation ratios, as shown in Table I. Compared to CPW resonators, this approach significantly reduces p_c, p_{ma}, and p_{sa} while leaving p_{ms} unchanged (Table I); hence, microstrip resonators are especially useful if the metal-substrate interface is the least lossy interface. This difference between the interfaces implies that it is possible to determine if the metal-substrate interface is dominant by comparing losses from CPW and microstrip resonators.

One might expect varying CPW resonator dimensions, as shown in Fig. 3, would determine dominant interfaces. For a fixed coplanar gap g, the loss decreases as $w^{-2/3}$ for trace widths $w \leq g$ and flattens off for $w > g$. Since larger widths increase loss by producing slotline modes, increasing radiation, and trapping flux in the center strip,[18] we characterized the case $w = g$, where loss is proportional to $1/w$. If the distance $w + 2g$ between the ground planes is fixed, minimal loss occurs at a characteristic impedance $Z_0 = 50$–60 Ω. However, in all three cases, the participation ratios for all four interface types have nearly the same dependence. Hence, varying dimensions can reduce loss but makes determining the dominant interface difficult.

One potential way to determine the key interfaces is by measuring the power dependence of the loss[10] since different
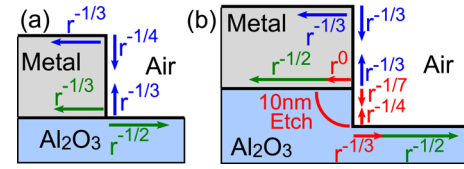

FIG. 2. (Color online) Electric field scaling on distances for CPW resonators. (a) is for an ordinary CPW, while (b) is for a CPW with the substrate etched in the coplanar gap. Arrows indicate for which distance r from the corner the electric field has the indicated scaling. As expected,[17] the field scales as $r^{-1/3}$ at metal edges in both cases and as $r^{-1/2}$ far from metal edges (b); a substantial fraction of the energy in both cases is concentrated at the corners. Etching the substrate in the coplanar gap reduces this dependence over a length corresponding to the etch depth, reducing the corner participation ratio.

interfaces have different field dependences from their corners (Fig. 2). For a 90° corner, where $E = E_0(r/r_0)^{-1/3}$, the surface participation ratio is[14]

$$\frac{p}{t\epsilon} = 3E_0^2 r_0 \left[\sqrt{1 + \frac{E_0^2}{E_s^2}} - \sqrt{\left(\frac{r_c}{r_0}\right)^{2/3} + \frac{E_0^2}{E_s^2}} \right], \quad (5)$$

where E_s is the saturation field, r_0 is a characteristic length, and r_c is a lower cutoff. For a metal edge, where $E = E_0(r/r_0)^{-1/2}$, the surface participation ratio is[14]

$$\frac{p}{t\epsilon} = 2E_0^2 r_0 \log \frac{1 + \sqrt{1 + \frac{E_0^2}{E_s^2}}}{\sqrt{\frac{r_c}{r_0}} + \sqrt{\frac{r_c}{r_0} + \frac{E_0^2}{E_s^2}}}, \quad (6)$$

which gives a logarithmic divergence. Comparing these results in Fig. 4, we find the $r^{-1/2}$ edge model has a much broader crossover with the drive field, while the $r^{-1/3}$ corner model is much closer to the sharp crossover of the simple TLS theory.[9] These models are also well described (Fig. 4) by the experimentally based fitting formula[9]

$$\frac{p}{t\epsilon} = \frac{cE_0^2 r_0}{[1 + 0.9c(E_0/E_s)^\alpha]^{1/\alpha}} \quad (7)$$

where $c = 3[1 - (r_c/r_0)^{1/3}]$. Here, $\alpha \approx 1.5$ for the $r^{-1/3}$ case, similar to an experimentally determined relation,[9] while
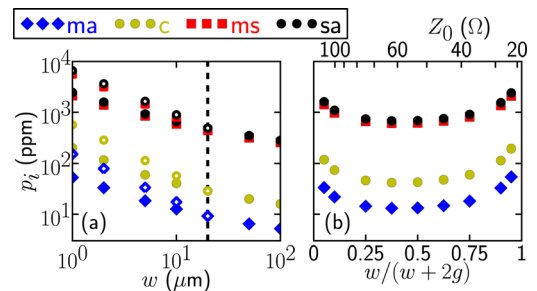

FIG. 3. (Color online) Geometric dependence of participation ratios for the metal-air (ma), corner (c), metal-substrate (ms), and substrate-air (sa) interfaces. We assume 3 nm surface dielectrics with $\epsilon_{ma} = \epsilon_{ms} = \epsilon_{sa} = 10$ along with $h = 100$ nm and $d = 10$ nm. (a) Open symbols are for $g = w$, where the loss decreases as $1/w$. Filled symbols are for fixed $g = 20$ μm (indicated by dashed line), where the loss decreases as $w^{-2/3}$. (b) Plot of loss vs. w for fixed $w + 2g = 40$ μm. Minimum loss occurs at a characteristic impedance $Z_0 = 50$–60 Ω. In all three cases, the participation ratios scale together, implying that changing geometrical parameters can not determine which interface is dominant.

TABLE I. Simulated losses for three resonator geometries.[14] Losses are calculated for $\epsilon_s = 10$ and surface dielectrics with $\epsilon = 10$, $t = 3$ nm, and loss tangent 0.002; dimensions are as in Fig. 1. Both coplanar waveguide (CPW) geometries, with identical dimensions, have similar metal-air (ma), metal-substrate (ms), and substrate-air (sa) losses, but etching the exposed substrate (Etched CPW) substantially reduces corner (c) loss. A microstrip geometry (with dielectric height s) has significantly less ma and sa losses than CPWs.

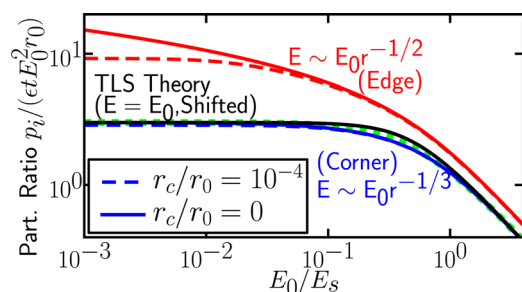| Type | Dimensions (μm) | | | | Loss $\times 10^6$ | | | |
	W	h	g	d	ma	ms	sa	c
CPW	5	0.1	2	0	0.10	6.13	4.02	1.32
Etched CPW	5	0.1	2	0.01	0.11	4.64	5.25	0.39
Microstrip	20	0.2	$s = 2$	0	0.02	6.60	0.79	0.38

FIG. 4. (Color online) Plot of surface participation ratio vs. electric field for different field dependences. The case $E \sim r^{-1/3}$, for a metal corner [Eq. (5)], has similar dependences if $r_c = 0$ (solid) or if $r_c/r_0 = 10^{-4}$ (dashed); both are similar to the TLS saturation theory case [$E = E_0$] and the simplified formula [Eq. (7) for $\alpha = 1.5$, dotted]. For the case $E \sim r^{-1/2}$, for a metal edge [Eq. (6)], the $r_c/r_0 = 10^{-4}$ curve (dashed) has a broader crossover, while the $r_c = 0$ (solid) case logarithmically diverges.

$\alpha \approx 0.75$ for the $r^{-1/2}$ case; this indicates that a corner, not an edge, dominated the experimental loss.

The surface loss model is partially validated by qualitatively explaining experimental results observed by others. For instance, HF-terminating a silicon substrate before growing a Nb film reduced the TLS loss to a third that of *in situ* plasma cleaning, confirming the importance of the metal-substrate interface.[12] While roughness in the coplanar gap did not affect their TLS loss, they substantially overetched into the substrate, so the substrate-air roughness experienced substantially lower fields. In addition, etching into the substrate reduced loss,[10] confirming the importance of the substrate-air interface.

Some prior experiments suggested that the metal-air interface is dominant but can be re-explained with the model presented here. We previously found Re resonators grown by molecular beam epitaxy had lower loss than sputter-grown Al resonators,[9] which was attributed to the metal-air interface. This may instead be from differences in surface preparation and cleanliness between the growth conditions, affecting the metal-substrate interface. In addition, Nb resonators on Si and sapphire substrates had similar losses and were more lossy than Al, Re, or TiN resonators; this was claimed to be from oxide formation at the metal-air interface.[11] However, oxygen diffuses into the Nb film from both the metal-substrate[19] and metal-air interfaces, giving much thicker interfaces which can dominate loss.

This model is not restricted to CPW resonators. The Nb cavity resonators of Brune, Raimond, and Haroche[20] have loss $1/Q = 2.4 \times 10^{-11}$. For typical parameters, the surface loss model gives a similar loss $\sim \tan \delta_{\text{ma}} p_{\text{ma}} / \epsilon_{\text{ma}} = 2.2 \times 10^{-11}$.

In conclusion, we have developed a model for the resonator loss from interfaces. We find that, for realistic values, the metal-substrate and substrate-air interfaces are dominant, with participation ratios of order 100 times that of the metal-air interface. The loss can therefore be reduced by improving the metal-substrate and substrate-air interfaces, using microstrips with clean dielectrics, and increasing dimensions.

[1]J. Schlaerth, A. Vayonakis, P. Day, J. Glenn, J. Gao, S. Golwala, S. Kumar, H. Leduc, B. Mazin, J. Vaillancourt, and J. Zmuidinas, J. Low Temp. Phys. **151**, 684 (2008).
[2]L. DiCarlo, J. M. Chow, J. M. Gambetta, Lev S. Bishop, B. R. Johnson, D. I. Schuster, J. Majer, A. Blais, L. Frunzio, S. M. Girvin, and R. J. Schoelkopf, Nature **460**, 240 (2009).
[3]F. Altomare, J. I. Park, K. Cicak, M. A. Sillanpää, M. S. Allman, D. Li, A. Sirois, J. A. Strong, J. D. Whittaker, and R. W. Simmonds, Nat. Phys. **6**, 777 (2010).
[4]M. Steffen, S. Kumar, D. DiVincenzo, G. Keefe, M. Ketchen, M. B. Rothwell, and J. Rozen, Appl. Phys. Lett. **96**, 102506 (2010).
[5]M. Ansmann, H. Wang, R. C. Bialczak, M. Hofheinz, E. Lucero, M. Neeley, A. D. O'Connell, D. Sank, M. Weides, J. Wenner, A. N. Cleland, and J. M. Martinis, Nature **461**, 504 (2009).
[6]H. Wang, M. Hofheinz, M. Ansmann, R. C. Bialczak, E. Lucero, M. Neeley, A. D. O'Connell, D. Sank, M. Weides, J. Wenner, and J. M. Martinis, Phys. Rev. Lett. **103**, 200404 (2009).
[7]H. Wang, M. Mariantoni, R. C. Bialczak, M. Lenander, E. Lucero, M. Neeley, A. O'Connell, D. Sank, M. Weides, J. Wenner, T. Yamamoto, Y. Yin, J. Zhao, J. M. Martinis, and A. N. Cleland, Phys. Rev. Lett. **106**, 060401 (2011).
[8]J. Gao, M. Daal, A. Vayonakis, S. Kumar, J. Zmuidzinas, B. Sadoulet, B. A. Mazin, P. K. Day, and H. G. Leduc, Appl. Phys. Lett. **92**, 152505 (2008).
[9]H. Wang, M. Hofheinz, J. Wenner, M. Ansmann, R. C. Bialczak, M. Lenander, E. Lucero, M. Neeley, A. D. O'Connell, D. Sank, M. Weides, A. N. Cleland, and J. M. Martinis, Appl. Phys. Lett. **95**, 233508 (2009).
[10]R. Barends, N. Vercruyssen, A. Endo, P. J. de Visser, T. Zijlstra, T. M. Klapwijk, P. Diener, S. J. C. Yates, and J. J. A. Baselmans, Appl. Phys. Lett. **97**, 023508 (2010).
[11]J. M. Sage, V. Bolkhovsky, W. D. Oliver, B. Turek, and P. B. Welander, J. Appl. Phys. **109**, 063915 (2011).
[12]D. S. Wisbey, J. Gao, M. R. Vissers, F. C. S. da Silva, J. S. Kline, L. Vale, and D. P. Pappas, J. Appl. Phys. **108**, 093918 (2010).
[13]J. Koch, T. M. Yu, J. M. Gambetta, A. A. Houck, D. I. Schuster, J. Majer, A. Blais, M. H. Devoret, S. M. Girvin, and R. J. Schoelkopf, Phys. Rev. A **76**, 042319 (2007).
[14]See supplementary material at http://dx.doi.org/10.1063/1.3637047 for derivations of the participation ratios, a discussion of interface thicknesses, an explanation of how simulations were performed, and a table of participation ratios for different geometries.
[15]COMSOL 3.6 (COMSOL AB: Stockholm, 2007).
[16]A. D. O'Connell, M. Ansmann, R. C. Bialczak, M. Hofheinz, N. Katz, E. Lucero, C. McKenney, M. Neeley, H. Wang, E. M. Weig, A. N. Cleland, and J. M. Martinis, Appl. Phys. Lett. **92**, 112903 (2008).
[17]J. D. Jackson, *Classical Electrodynamics*, 3rd ed. (Wiley, Hoboken, 1999).
[18]C. Song, T. W. Heitmann, M. P. DeFeo, K. Yu, R. McDermott, M. Neeley, J. M. Martinis, and B. L. T. Plourde, Phys. Rev. B **79**, 174512 (2009).
[19]C. Sürgers and H. v. Löhneysen, Appl. Phys. A **54**, 350 (1992).
[20]S. Gleyzes, S. Kuhr, C. Guerlin, J. Bernu, S. Déléglise, U. B. Hoff, M. Brune, J.-M. Raimond, and S. Haroche, Nature **446**, 297 (2007).